DOI: 10.1002/ejic.200501006

Structural Studies of β-Cyclodextrin and Permethylated β-Cyclodextrin Inclusion Compounds of Cyclopentadienyl Metal Carbonyl Complexes

Susana S. Braga,[a] Filipe A. Almeida Paz,[a] Martyn Pillinger,[a] João D. Seixas,[b,c] Carlos C. Romão,*[b,c] and Isabel S. Gonçalves*[a]

Keywords: Ab initio calculations / Cyclodextrins / Inclusion compounds / Iron / Molybdenum / Sandwich complexes

[CpM(CO)$_n$Cl] complexes with M = Fe (n = 2) and Mo (n = 3) have been immobilised in plain β-cyclodextrin (β-CD) and permethylated β-CD (TRIMEB) by methods tailored according to the stabilities and solubilities of the individual components. Four adducts were obtained with a 1:1 host/guest stoichiometry. The compounds were studied by powder X-ray diffraction (XRD), thermogravimetric analysis (TGA), $^{13}C\{^1H\}$ CP/MAS NMR and FTIR spectroscopy. A comparison of the experimental powder XRD data for the TRIMEB/[CpMo(CO)$_3$Cl] inclusion compound with reference patterns revealed that the crystal packing is very similar to that reported previously for a TRIMEB/ethyl laurate inclusion compound. The unit-cell parameters refined to a = 14.731, b = 22.476, c = 27.714 Å (volume = 9176.3 Å^3), and the space group was confirmed as $P2_12_12_1$. A hypothetical structural model of the inclusion compound was subsequently obtained by global optimisation using simulated annealing.

Introduction

Cyclodextrins (CDs) are water-soluble cyclic oligosaccharides that are capable of forming inclusion compounds with a wide range of organic molecules, inorganic ions and metallo-organic species.[1] Suitable guests include transition metal complexes and organometallic compounds bearing hydrophobic ligands such as cyclopentadienyl (Cp = η^5-C_5H_5) and η^6-arene groups.[2] With these ligands, the weaker categories of non-covalent bonding, such as van der Waals and charge-transfer interactions, assume considerable importance. CDs are known to bind ferrocene and its derivatives,[3] metallocene dihalides,[4] aromatic ruthenium complexes,[5] mixed-sandwich complexes such as [(η^5-C_5H_5)Fe(η^6-C_6H_6)](PF_6),[6] and half-sandwich complexes such as [CpFe(CO)$_2$X] (X = Cl, Me, CN),[7] [CpFe(CO)$_2$-NH_3](PF_6),[8] [CpMn(CO)$_3$],[9] [(η^6-C_6H_6)Cr(CO)$_3$],[10] [Cp′Mo(η^3-C_3H_5)(CO)$_2$],[11] [Cp′Mo(η^3-C_6H_7)(CO)$_2$] and [Cp′Mo(η^4-C_6H_8)(CO)$_2$](BF_4) (Cp′ = Cp, Ind).[12] Encapsulated metallo-organic complexes often exhibit markedly different physical and chemical characteristics compared to the bulk material, for example in their nonlinear optical properties,[13] electrochemical behaviour,[3b,3g,3i,3j,14] ligand substitution/insertion reactions,[7a,7b] and catalysis.[15] In the present work, we describe the synthesis and solid-state characterisation of inclusion compounds formed between the cyclopentadienyl metal carbonyl complexes [CpFe(CO)$_2$Cl] (**1**) and [CpMo(CO)$_3$Cl] (**2**) (Figure 1) and unmodified β-cyclodextrin and 2,3,6-tri-*O*-methyl-β-CD (TRIMEB). The encapsulation of the tricarbonylmolybdenum complex is of particular interest because this molecule is a precursor to the dioxomolybdenum(VI) complex [CpMoO$_2$Cl], which has been shown to be a very effective catalyst for the epoxidation of olefins using *tert*-butyl hydroperoxide as the oxidising agent.[16]

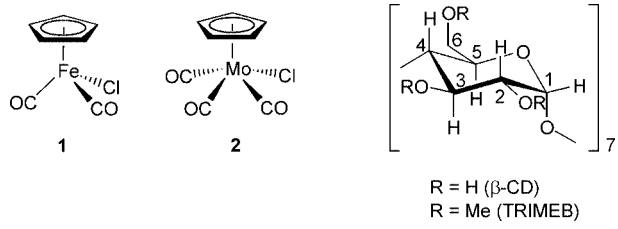

Figure 1. Guests and hosts used in this work.

Among the organometallic–cyclodextrin inclusion compounds described in the literature, only a few have been successfully characterised by single-crystal X-ray diffraction,[3e,3f,5,6] mainly because of the difficulty in preparing crystals of appropriate size that exhibit stability under the X-ray beam over the period of data collection. Useful structural information can, however, be obtained through a combination of other techniques such as powder XRD and NMR spectroscopy.[17–19] In particular, Caira described a

[a] Department of Chemistry, CICECO, University of Aveiro, 3810-193 Aveiro, Portugal
Fax: +351-234-370084
E-mail: igoncalves@dq.ua.pt
[b] Instituto de Tecnologia Química e Biológica da Universidade Nova de Lisboa,
Quinta do Marquês, EAN, Apt. 127, 2781-901 Oeiras, Portugal
[c] Alfama, Research and Development of Pharmaceutical Drugs, Ltd.,
IBET, Apartado 12, 2781-901 Oeiras, Portugal

few years ago a reliable empirical technique based on the visual comparison of X-ray powder patterns, which can almost unambiguously identify the type of crystal-packing arrangement of CD molecules in a typical host–guest inclusion compound.[17] This method can be envisaged as a "manual" (in some cases not very effective) direct-space approach to finding a hypothetical structural model. Even though it gives a rather reasonable first approach, this technique is also limited in its essence as it cannot explore all of the possible combinations in direct space. In this paper, we use conventional powder X-ray data, in combination with the technique proposed by Caira, to produce a hypothetical structural model of the inclusion compound TRIMEB·[CpMo(CO)$_3$Cl], obtained by global optimisation using simulated annealing. The calculations were performed using the recently developed FOX program,[20,21] which has proven to be a reliable, fast and robust software package for the solution of many different types of compounds.[22–26] This kind of ab initio model idealisation is unusual among compounds typically composed of light atoms (such as carbon, hydrogen and oxygen), and, to the best of our knowledge, is completely unprecedented among cyclodextrin inclusion compounds.

Results and Discussion

The relative solubilities of β-CD, TRIMEB, and the complexes [CpFe(CO)$_2$Cl] (**1**) and [CpMo(CO)$_3$Cl] (**2**) determined the method used for the preparation of the respective inclusion compounds. An initial CD/complex molar ratio of 1:1 was always used. The iron complex **1** is slightly water soluble, and so the encapsulations were carried out using a mixture of water and ethanol. The compound β-CD·[CpFe(CO)$_2$Cl] (**3**) precipitated as an orange microcrystalline solid upon slow cooling of a hot water/ethanol solution. The high solubility of the modified cyclodextrin TRIMEB meant that the corresponding adduct, TRIMEB·[CpFe(CO)$_2$Cl] (**4**), could only be isolated by complete evaporation of the solvents. For the molybdenum complex **2**, dichloromethane had to be used to solubilise the guest. β-CD inclusion was achieved by mixing a dichloromethane solution of **2** with an aqueous solution of β-CD. After stirring at 40 °C for 2 h, a microcrystalline brick-red precipitate formed at the interface between the two solutions, designated as β-CD·[CpMo(CO)$_3$Cl] (**5**). Inclusion of the molybdenum complex **2** in TRIMEB was performed by dissolving the guest in a dichloromethane solution of the host followed by vacuum-drying to isolate TRIMEB·[CpMo(CO)$_3$Cl] (**6**). This uncommon technique works particularly well for the methylated cyclodextrin TRIMEB due to its high solubility in organic solvents. In fact, the same method has been successfully used by some of us in previous work.[27] Elemental analysis of compounds **3**–**6** confirmed that the final host/guest molar ratios were close to 1:1.

X-ray diffraction studies allow the identification of true inclusion complexes of cyclodextrins, mainly based on the empirical evidence that the powder XRD patterns of these complexes should be clearly distinct from those obtained by the superimposition of the diffractograms of each individual component.[1b] Figure 2 shows the patterns for complexes **1** and **2**, β-CD, and the adducts **3** and **5**. The diffractograms for the adducts are clearly different from the sum of the individual patterns of β-CD and either the iron complex **1** or the molybdenum complex **2**. For compound **3**, the overall pattern matches reasonably well with the reference pattern reported by Caira for the isostructural series characterised by channel-type packing of β-CD dimers (C_2 space group).[17] This type of packing has been previously identified in several β-CD inclusion complexes of organometallic molecules, such as ferrocene derivatives,[3k] mixed-sandwich complexes,[6] and half-sandwich molybdenum carbonyl complexes.[11,12] Most of the reflections in the powder XRD pattern of compound **5** match those present in the corresponding pattern for the parent β-CD hydrate, even though substantial changes in relative intensities are markedly visible along with some slight displacements in the 2θ values. The reflection centred at about 4.5° 2θ is characteristic of cage-type packing, as observed for β-CD hydrate or β-CD inclusion complexes of relatively small guests.[17] The existence of this type of crystal packing for compound **5** would therefore be surprising, although it is known that a molecule at least as large as benzyl alcohol can be accommodated by the host without a change in the packing arrangement.[17]

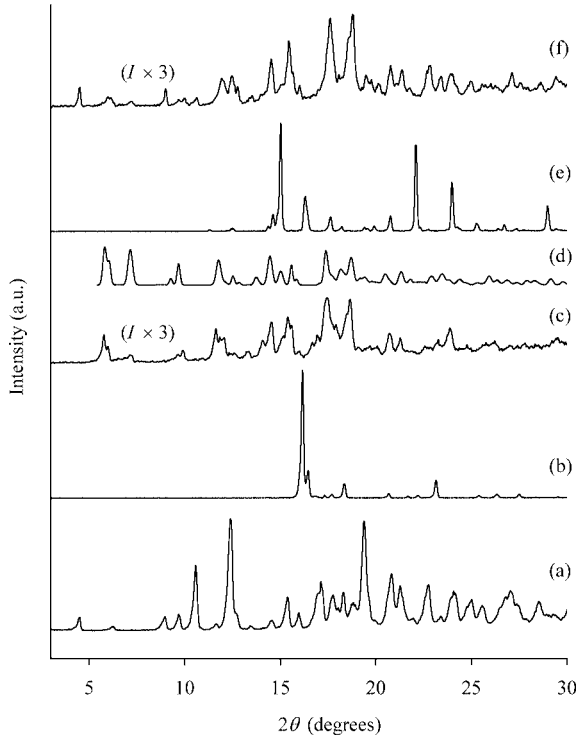

Figure 2. Powder XRD patterns of (a) β-CD hydrate, (b) [CpFe(CO)$_2$Cl] (**1**), (c) the inclusion compound β-CD·[CpFe(CO)$_2$Cl] (**3**), (d) a channel model,[16] (e) [CpMo(CO)$_3$Cl] (**2**) and (f) the inclusion compound β-CD·[CpMo(CO)$_3$Cl] (**5**).

Figure 3 shows the powder XRD patterns for complexes **1** and **2**, TRIMEB, and adducts **4** and **6**. Compound **4** is poorly crystalline, making it difficult to deduce the type of crystal packing arrangement. Nevertheless, a comparison of this pattern with those for the iron complex **1** and the parent TRIMEB indicates that a true inclusion compound has been isolated. The adduct TRIMEB·[CpMo(CO)$_3$Cl] (**6**) exhibits a better defined diffractogram, which could also be attributed to a new phase corresponding to a true inclusion compound. A careful inspection of this pattern suggests that the crystal packing should share close similarities with that found by Mentzafos et al. for a 1:1 inclusion compound comprising TRIMEB and ethyl laurate (in which the macrocycles are arranged along the *b* axis in a zigzag mode to form a distorted column structure).[28] This allowed us to perform a more in-depth structural evaluation using ab initio calculations. As typically observed for this type of compounds, the overall crystallinity of TRIMEB·[CpMo(CO)$_3$Cl] (**6**) is low due to structural orientation disorder of the host and/or the guest molecules, and the existence of several solvent molecules also highly affected by thermal disorder. Compound **6** diffracts very weakly at high angles and the diffractogram is generally characterised by poorly resolved lines (with large full-width-at-half-maximum). This creates, a priori, several limitations for a typical ab initio structural determination, and several approximations based on empirical evidence had to be taken into account (see below).

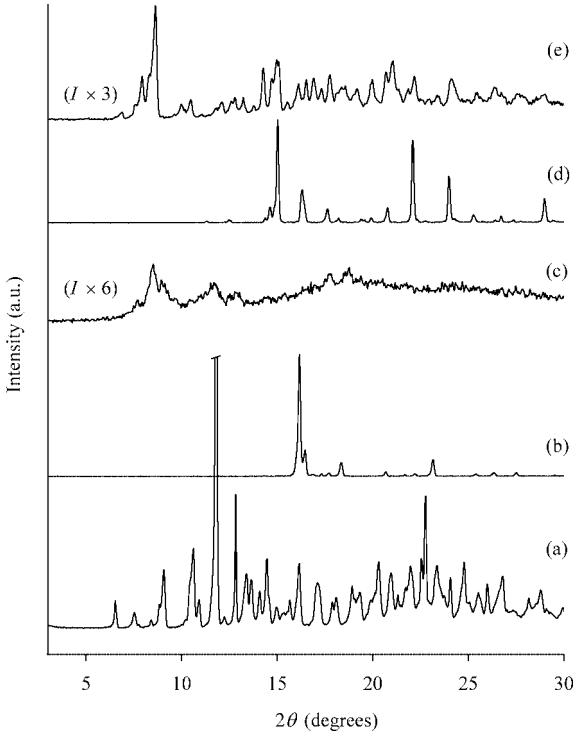

Figure 3. Powder XRD patterns of (a) TRIMEB, (b) [CpFe(CO)$_2$Cl] (**1**), (c) the inclusion compound TRIMEB·[CpFe(CO)$_2$Cl] (**4**), (d) [CpMo(CO)$_3$Cl] (**2**) and (e) the inclusion compound TRIMEB·[CpMo(CO)$_3$Cl] (**6**).

The ab initio determination of a hypothetical structural model for the inclusion compound TRIMEB·[CpMo(CO)$_3$Cl] (**6**) started by comparing the experimental data with the TRIMEB/ethyl laurate model compound, which has the Cambridge Structural Database (CSD)[29,30] refcode PINMAA [crystal data: a = 14.796(2), b = 22.444(6), c = 27.720(8) Å, V = 9205.03 Å^3, and space group $P2_12_12_1$]. Collected data were examined using the software package CHECKCELL,[31] and the unit-cell parameters refined to a = 14.731, b = 22.476, and c = 27.714 Å (volume = 9176.3 Å^3), using 33 reflections for the CELREF subroutines.[32] By cross-examining the collected powder XRD pattern with the refined cell parameters, the space group of $P2_12_12_1$ for the inclusion compound **6** was unambiguously confirmed using CHECKCELL.

The modelling of compound **6** using FOX[20,21] started by assuming that the interactions between the guest [CpMo(CO)$_3$Cl] and the host TRIMEB molecules are mainly weak (van der Waals and hydrogen-bonding interactions) and mediated by close-packing principles. We assumed that the molecular geometries of the individual molecules remain relatively unchanged upon interaction to form the inclusion complex. In this case, FOX is particularly robust as individual molecules can be added as mathematical objects in the form of a Fenske–Hall Z-matrix, thus retaining some tacit knowledge of their geometry for the optimisation algorithm. Moreover, as the guest molecule contains a heavy atom (Mo), whose electron density contrasts well with the smeared-out density coming from the organic component, we assumed that the crystallographic position of [CpMo(CO)$_3$Cl] would be easily determined from the powder XRD pattern.

Firstly, the atomic coordinates of [CpMo(CO)$_3$Cl] were taken from the structure reported by Bueno et al. (deposited in the CSD with the refcode CPDMOC01),[33] and a Fenske–Hall Z-matrix (without hydrogen atoms) was created using BABEL.[34] The pivot atom was selected to be the central Mo in order to facilitate the mobility of the rigid molecule inside the unit cell. A Monte Carlo optimisation (using the optimised parallel tempering algorithm), in which the parameters of the Z-matrix were fixed (i.e., the molecule was treated as a rigid body), was launched in FOX and, after nearly 1,300,000 movements, the initial location of the crystallographically independent [CpMo(CO)$_3$Cl] complex was found (calculated weighted residual of R_{wp} = 0.412). Starting from random initial positions, individual optimisations converged to nearly the same final crystallographic location, with comparable R_{wp} factors. Figure 4 (b) shows the simulated powder XRD pattern for the hypothetical unit cell containing just the [CpMo(CO)$_3$Cl] complexes.

In the next stage of the global optimisation, the position of the [CpMo(CO)$_3$Cl] moieties was fixed and a second crystallographic object composed of a Fenske–Hall Z-matrix (also without hydrogen atoms) of the cyclodextrin TRIMEB, as reported by Mentzafos et al.,[28] was added to the unit cell. In the subsequent Monte Carlo optimisation steps using FOX (once again using the more efficient parallel tempering algorithm), the PINMAA residue was allowed to

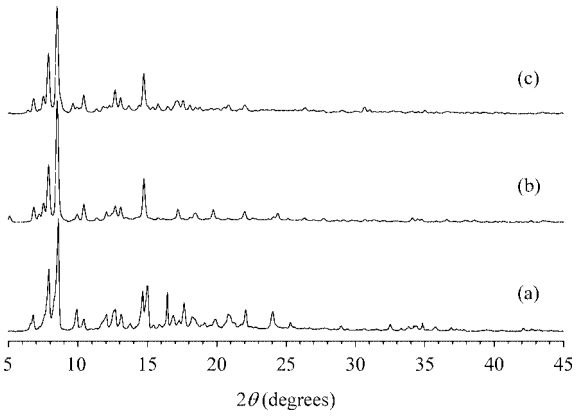

Figure 4. Powder XRD patterns of: (a) the as-synthesised inclusion compound TRIMEB·[$CpMo(CO)_3Cl$] (**6**), (b) the unit cell containing just the individual [$CpMo(CO)_3Cl$] complexes and (c) the hypothetical structural model for the inclusion compound **6**.

freely move as a rigid body and, after just four million moves, the model converged to that shown in Figure 5. Figure 4 (c) shows the simulated powder XRD pattern with a calculated weighted residual of R_{wp} = 0.386. Apart from the general low crystallinity of the inclusion complex, the powder pattern is also affected by textural effects such as preferred orientation. To minimise such effects a refineable March–Dollase correction[35,36] was applied in FOX. The model obtained using the Monte Carlo optimisation clearly proves the existence of a true inclusion complex, with the final convergence being achieved without the use of any antibump restraints. Since this model was obtained by treating the molecules as rigid entities, some groups of atoms are closer together than they would be in a real crystal structure. This is particularly evident for the methyl groups of TRIMEB, which, in some cases, nearly overlap. Such "structural errors" could be eliminated by performing a Rietveld refinement in the present model. However, as high-resolution powder XRD data were not available due to the low crystallinity of the material, and probably could only be obtained using synchrotron radiation, preliminary studies using FULLPROF[37] did not produce the expected results (data not shown).

Thermogravimetric analysis was also useful for the recognition of inclusion complex formation in compounds **3**–**6** (Figure 6). The β-CD adducts β-CD·[$CpFe(CO)_2Cl$] (**3**) and β-CD·[$CpMo(CO)_3Cl$] (**5**) exhibit a step from room temperature up to about 65 °C, assigned to the removal of water molecules located in the β-CD cavities, and also in the interstices between the macrocycles. The corresponding weight losses are 10.7% for **3** and 6.2% for **5**, which are in agreement with the microanalysis results and indicate that the approximate number of water molecules per β-CD molecule in **3** and **5** are eight and six, respectively. For comparison, plain β-CD hydrate shows a similar well-defined step from room temperature up to about 80 °C (not shown), with a mass loss of 14.6% (11 water molecules per β-CD molecule). The reduction in the number of water molecules

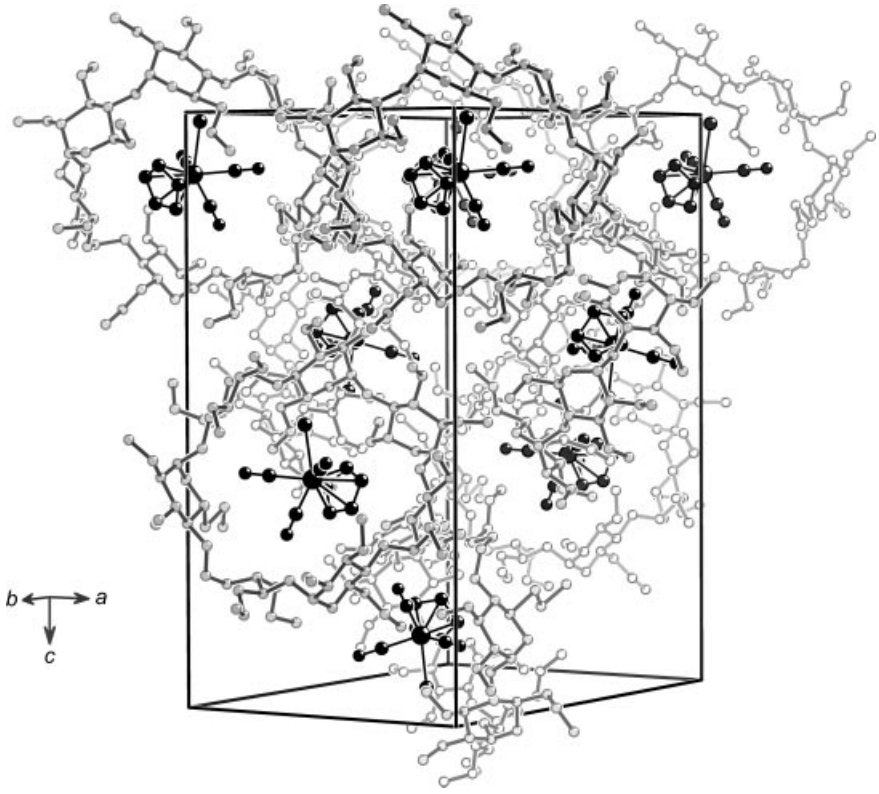

Figure 5. Unit cell contents, viewed in perspective towards the (1 7 0) plane, of the Monte Carlo optimised structural model of the inclusion compound TRIMEB·[$CpMo(CO)_3Cl$] (**6**). TRIMEB and [$CpMo(CO)_3Cl$] residues are represented with grey- and black-filled bonds, respectively.

per β-CD molecule in the inclusion compounds is consistent with at least partial occupation of the β-CD cavities by the hydrophobic organometallic guests. After the dehydration step, the TG curves for **3** and **5** are very similar. There is a gradual mass loss in the temperature range of 65–200 °C (7.8% for **3** and 9.8% for **5**), attributed to the loss of CO and/or Cl ligands from the included guest molecules (since plain β-CD hydrate exhibits insignificant mass loss in the temperature range of 80–200 °C). The corresponding steps for the non-included complexes **1** and **2** are much more abrupt (not shown): 16.3% between 90 and 120 °C for **1**, and 23.6% between 100 and 160 °C for **2**. Finally, the host molecules in the two inclusion compounds start to decompose at about 205 °C, while plain β-CD hydrate starts to decompose around 270 °C. This difference is attributed to the promoting effects of iron and molybdenum on the decomposition of β-cyclodextrin, and is further evidence for the existence of a significant host–guest interaction in the inclusion compounds.[10] A similar result was obtained for the TRIMEB inclusion compounds TRIMEB·[CpFe(CO)$_2$Cl] (**4**) and TRIMEB·[CpMo(CO)$_3$Cl] (**6**). Thus, while pure TRIMEB starts to melt and decompose at about 175 °C (not shown), compounds **4** and **6** start at 135 and 150 °C, respectively (Figure 6). In the low-temperature range of the thermogram compound **6** exhibits a weight loss between 75 and 130 °C (2.8%), presumably due to the partial loss of CO and/or Cl ligands from the included guest molecules. No such step is evident for compound **4**, and only a minor mass loss of about 1% is observed from room temperature up to the onset of decomposition. Finally, it is worth noting that the residual masses at 500 °C are 6.1% for the inclusion compounds containing the Fe complex and 9.5% for the compounds containing the Mo complex.

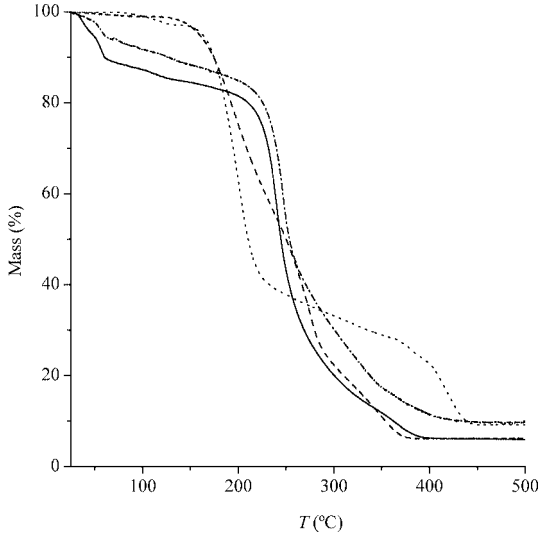

Figure 6. TGA curves of the inclusions compounds β-CD·[CpFe(CO)$_2$Cl] (**3**) (——), TRIMEB·[CpFe(CO)$_2$Cl] (**4**) (– – –), β-CD·[CpMo(CO)$_3$Cl] (**5**) (– · – ·), and TRIMEB·[CpMo(CO)$_3$Cl] (**6**) (· · · · ·).

The $^{13}C\{^1H\}$ CP/MAS NMR spectra of complexes **1** and **2**, and their corresponding inclusion compounds with β-CD and TRIMEB, are shown in Figure 7 for the [CpFe(CO)$_2$Cl] series and in Figure 8 for the [CpMo(CO)$_3$Cl] series. Plain β-CD hydrate exhibits a complex $^{13}C\{^1H\}$ CP/MAS NMR spectrum (not shown), with multiple sharp resonances for each type of carbon atom. These features have been correlated with different torsion angles about the α(1→4) linkages,[38] and with torsion angles describing the orientation of the hydroxy groups.[39] Upon inclusion to give β-CD·[CpFe(CO)$_2$Cl] (**3**) and β-CD·[CpMo(CO)$_3$Cl] (**5**), the resonances due to the C1, C4, C2,3,5, and C6 host carbon atoms (Figure 1) appear mainly as single broad peaks, with little or no structure, centred around δ = 104, 81, 73, and 61 ppm, respectively. Furthermore, the dispersion in the chemical shift for each signal (i.e., the chemical-shift range that comprises all of the resonances from the same carbon atom in distinct glycosidic units) decreases with respect to the β-CD spectrum. These observations are typically attributed to a symmetrisation of the β-CD macrocycle, that is, the encapsulation of the guest molecule induces the ring to adopt a less distorted conformation, with each glucose unit in a more similar environment.[3k,3l,4b,7d,11,12,40] For the inclusion compound **3** (Figure 7), the Cp carbon atoms of the guest molecule give rise to one weak resonance at δ = 89.2 ppm, which is shifted downfield by 2.5 ppm relative to the resonance for non-included [CpFe(CO)$_2$Cl] (**1**). The Cp carbon atoms of the mo-

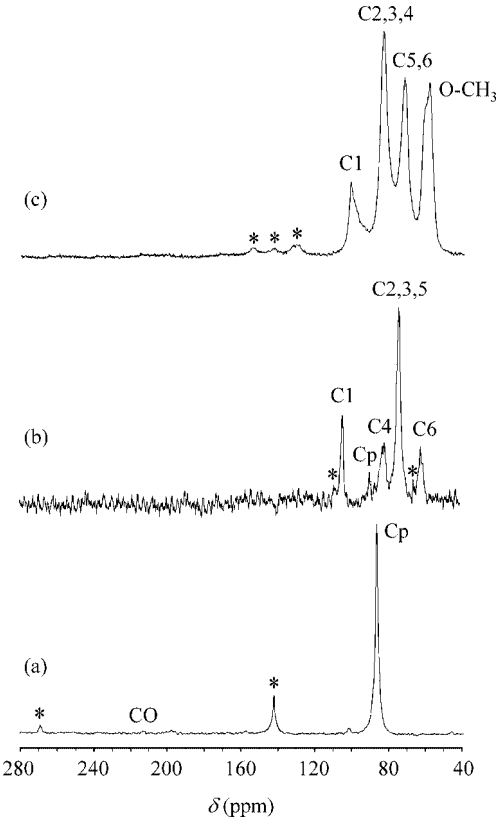

Figure 7. Solid-state $^{13}C\{^1H\}$ CP/MAS NMR spectra of (a) [CpFe(CO)$_2$Cl] (**1**), (b) the inclusion compound β-CD·[CpFe(CO)$_2$Cl] (**3**) and (c) the inclusion compound TRIMEB·[CpFe(CO)$_2$Cl] (**4**). Spinning sidebands are denoted by asterisks.

lybdenum complex in **5** give rise to two resolved peaks at δ = 94.8 and 96.1 ppm, which are shifted slightly upfield relative to the sharp line exhibited by non-included [$CpMo(CO)_3Cl$] (**2**) (Figure 8). The presence of two peaks may mean that there are two distinct inclusion modes for the guest molecule, comprising, for example, different orientations of the guest relative to the host and/or different degrees of penetration of the guest in the host cavity.

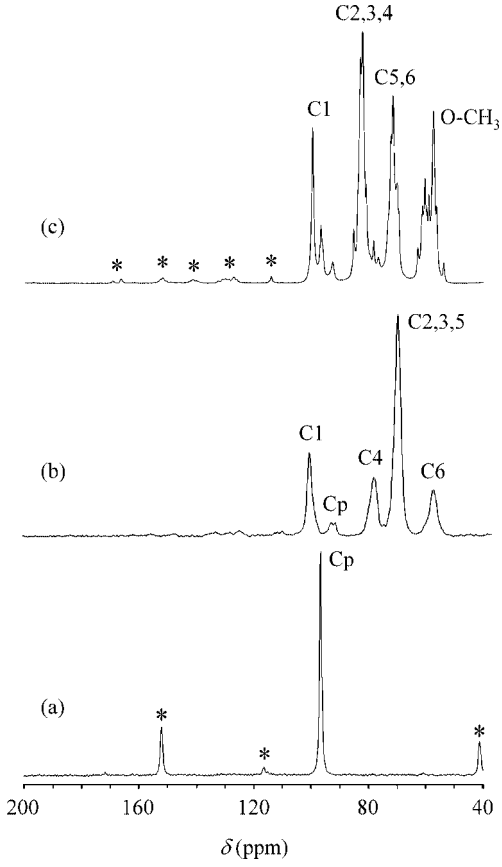

Figure 8. Solid-state $^{13}C\{^1H\}$ CP/MAS NMR spectra of (a) [$CpMo(CO)_3Cl$] (**2**), (b) the inclusion compound β-CD·[$CpMo(CO)_3Cl$] (**5**) and (c) the inclusion compound TRIMEB·[$CpMo(CO)_3Cl$] (**6**). Spinning sidebands are denoted by asterisks.

Like plain β-CD hydrate, the $^{13}C\{^1H\}$ CP/MAS NMR spectrum of TRIMEB also shows multiple resonances for each type of carbon atom (not shown).[27] This is because the host assumes a severely collapsed conformation in the solid state, which minimises the hydrophobic cavity in the absence of a hydrophobic guest. This multiplicity is lost for the inclusion compound TRIMEB·[$CpFe(CO)_2Cl$] (**4**) and only broad peaks are observed, indicating a change in the conformation of the host macrocycle (Figure 7).[27,41] The spectrum for the inclusion compound TRIMEB·[$CpMo(CO)_3Cl$] (**6**) is slightly different, exhibiting several resolved lines for each type of carbon atom (Figure 8). This could be related to the fact that the overall crystallinity of compound **6** is higher than that for compound **4**, as evidenced by powder XRD. For compound **6**, at least seven resonances are discernible for the methyl carbon atoms, indicating that these groups exist in several different well-defined environments. The expected Cp resonances for the guest molecules in compounds **4** and **6** cannot be confidently assigned due to overlap with the resonances for the C1 carbon atoms of the host. Also, for all of the inclusion compounds studied, even with a contact time of 2 ms, it was not possible to clearly identify the resonances (masked in the background) for the CO groups of the guest molecules. The presence of these groups was confirmed by IR spectroscopy. Thus, in addition to the intense and typical bands of the cyclodextrin hosts, the spectra contain strong bands in the CO stretching region (1940–2060 cm^{-1}). As expected, two bands are observed for compounds **3** and **4**, while three bands were identified for compounds **5** and **6**. These are slightly shifted relative to the corresponding bands for the non-included complexes **1** and **2** in the solid state. The spectra for the inclusion compounds also contain bands in the range 800–850 cm^{-1} (out-of-plane CH deformation of the Cp ring) and 1420–1430 cm^{-1} (C–C stretching vibration of the Cp ring).

Concluding Remarks

Inclusion compounds comprising cyclodextrins and half-sandwich complexes of iron and molybdenum have been prepared with a 1:1 host-to-guest stoichiometry and characterised in the solid state by various techniques. The results support the existence of true inclusion compounds. By reference to previous molecular modelling and crystallographic studies of related organometallic–cyclodextrin adducts, it is reasonable to conclude that the interaction geometries in the studied compounds probably involve insertion of the Cp ligands inside the host cavities. The ab initio determination of a hypothetical structural model for the inclusion compound TRIMEB·[$CpMo(CO)_3Cl$] using X-ray studies in direct space has afforded a reliable structural model which is, on the one hand, in good agreement with the results obtained using the other techniques (such as TGA and solid-state NMR) and, on the other, a systematic implementation of the empirical technique previously described by Caira.[17] The low crystallinity of the sample under study, largely reflected in the generally poorly resolved powder XRD pattern, prevents a more precise structural refinement. However, we are currently applying the strategies described in this manuscript to other more crystalline cyclodextrin inclusion compounds. As mentioned in the introduction, oxidative decarbonylation of [$CpMo(CO)_3Cl$] yields a dioxomolybdenum(VI) complex which is an active catalyst for the epoxidation of olefins. We are investigating the effect that CD encapsulation has on the reactivity of the tricarbonyl complex towards oxidative decarbonylation, that is, the possibility of forming a CD·[$CpMoO_2Cl$] complex. Molecular encapsulation of the tricarbonyl complex with TRIMEB may be advantageous in several ways from a catalytic point of view, such as enhancing the solubility of the pre-catalyst in different solvents, and improving the stability of the resultant dioxomolybdenum(VI) complex.

Experimental Section

General Remarks: β-CD was kindly donated by Laboratoires La Roquette (France), and heptakis-2,3,6-tri-*O*-methyl-β-CD was obtained from Fluka. All air-sensitive operations were carried out using standard Schlenk techniques under nitrogen. Solvents were dried by standard procedures, distilled under nitrogen or argon, and kept over 4-Å molecular sieves. Microanalyses for CHN were performed at the ITQB, Oeiras, Portugal (by C. Almeida), and Fe/Mo were determined by ICP-OES at the Central Laboratory for Analysis, University of Aveiro (by E. Soares). TGA studies were carried out using a Shimadzu TGA-50 system at a heating rate of 5 °C min^{-1} under air. Powder XRD data were collected at ambient temperature on an X′Pert MPD Philips diffractometer (Cu-K_α X-radiation) with a curved graphite monochromator. Routine examination of compounds **1**–**6** was performed with quick scans with variable slit opening (Figures 2 and 3). Data for the structure optimisation (Figure 4) were collected with a fixed divergence slit of 1/8°, and a flat plate sample holder, in a Bragg–Brentano parafocusing optics configuration. Intensity data were collected by the step counting method (step 0.03° and time 35 s) in the $5° \leq 2\theta \leq 45°$ range. Infrared spectra were recorded with a Unican Mattson Mod 7000 FTIR spectrophotometer. $^{13}C\{^1H\}$ CP/MAS NMR spectra were recorded at 125.72 MHz on a (11.7 T) Bruker Avance 500 spectrometer, with an optimised π/2 pulse for ^1H of 4.5 μs, 2-ms contact time, a spinning rate of 7 kHz and 12-s recycle delays. Chemical shifts are quoted in parts per million from tetramethylsilane. The complexes $[CpFe(CO)_2Cl]$ (**1**) and $[CpMo(CO)_3Cl]$ (**2**) were prepared as described in the literature,[42] and characterised by elemental analysis and FTIR spectroscopy.

β-CD·[CpFe(CO)$_2$Cl] (3): A solution of β-CD (110 mg, 0.09 mmol) in water (2 mL) at 70 °C was added dropwise to a solution of $[CpFe(CO)_2Cl]$ (**1**; 20 mg, 0.09 mmol) in ethanol (1 mL), and the resultant brick-red solution was stirred for 30 min. After cooling slowly inside a Dewar flask, an orange microcrystalline precipitate was formed, which was separated from the mother liquor and dried. $(C_{42}H_{70}O_{35})\cdot(C_7H_5ClFeO_2)\cdot 8H_2O$ (1491.5): calcd. C 39.46, H 6.15, Fe 3.74; found C 39.52, H 6.54, Fe 3.31. TGA up to 65 °C revealed a sample weight loss of 10.7% (calcd: for loss of 8 H_2O, 9.7%). FTIR (KBr): $\tilde{\nu}$ = 3375 cm^{-1} vs, 2967 sh, 2925 m, 2040 s, 1995 s, 1639 m, 1429 m, 1370 m, 1334 m, 1305 m, 1245 w, 1206 w, 1157 s, 1103 s, 1080 s, 1054 vs, 1027 vs, 1003 vs, 945 m, 937 m, 860 m, 841 m, 836 m, 757 m, 703 m, 669 m, 606 m, 635 m, 592 m, 576 m, 542 sh, 504 w, 476 m, 442 w, 412 m, 355 w. $^{13}C\{^1H\}$ CP/MAS NMR: δ = 104.2 (β-CD, C1), 89.2 (guest, Cp), 81.0 (β-CD, C4), 73.0 (β-CD, C2,3,5), 61.3 ppm (β-CD, C6).

TRIMEB·[CpFe(CO)$_2$Cl] (4): A solution of TRIMEB (1.55 g, 1.08 mmol) and $[CpFe(CO)_2Cl]$ (**1**; 230 mg, 1.08 mmol) in a mixture of water and ethanol (10 + 10 mL) was stirred for 1 h. The solution was then evaporated to dryness to give an orange solid. $(C_{63}H_{112}O_{35})\cdot(C_7H_5ClFeO_2)\cdot 2H_2O$ (1678.0): calcd. C 50.11, H 7.27, Fe 3.33; found C 50.00, H 6.08, Fe 3.34. FTIR (KBr): $\tilde{\nu}$ = 3480 cm^{-1} m, 2984 s, 2931 s, 2841 m, 2050 s, 2004 s, 1792 w, 1751 w, 1717 m, 1623 m, 1418 sh, 1460 m, 1404 sh, 1368 m, 1324 m, 1304 m, 1196 sh, 1164 vs, 1141 vs, 1107 vs, 1087 vs, 1071 vs, 1035 vs, 968 s, 950 sh, 937 s, 907 m, 857 m, 785 vw, 755 m, 706 m, 605 m, 596 w, 567 m, 548 m, 470 vw, 376 vw, 348 m. $^{13}C\{^1H\}$ CP/MAS NMR: δ = 99.7 (TRIMEB, C1), 82.4 (TRIMEB, C2,3,4 and overlapping guest Cp), 71.3 (TRIMEB, C5,6), 58.1 ppm (TRIMEB, O-CH_3).

β-CD·[CpMo(CO)$_3$Cl] (5): A solution of $[CpMo(CO)_3Cl]$ (**2**; 32 mg, 0.12 mmol) in dichloromethane (1 mL) was added to a solution of β-CD (150 mg, 0.12 mmol) in water (4 mL) at 40 °C, and the resultant biphasic mixture was stirred for 2 h. During this period, a pale brick-red precipitate formed at the interface between the two solutions. The solid was recovered, washed with dichloromethane (2 mL) and water (10 mL), and dried. $(C_{42}H_{70}O_{35})\cdot(C_8H_5MoO_3Cl)\cdot 6H_2O$ (1523.6): calcd. C 39.42, H 5.76, Mo 6.30; found C 39.50, H 6.03, Mo 5.45. TGA up to 65 °C revealed a sample weight loss of 6.2% (calcd: for loss of 6H_2O, 7.1%). FTIR (KBr): $\tilde{\nu}$ = 3345 cm^{-1} vs, 2923 s, 2853 sh, 2044 s, 1968 s, 1944 s, 1642 m, 1426 m, 1380 m, 1369 m, 1334 m, 1248 m, 1202 m, 1157 s, 1104 s, 1082 s, 1055 vs, 1028 vs, 1004 s, 945 m, 937 m, 860 m, 837 sh, 827 w, 759 m, 703 m, 606 m, 594 m, 576 m, 528 m, 499 vw, 474 w, 445 w, 435 w, 407 m, 404 sh, 378 vw, 359 m, 358 sh. $^{13}C\{^1H\}$ CP/MAS NMR: δ = 104.0 (β-CD, C1), 96.1, 94.8 (guest, Cp), 81.5 (β-CD, C4), 73.0 (β-CD, C2,3,5), 60.6 ppm (β-CD, C6).

TRIMEB·[CpMo(CO)$_3$Cl] (6): $[CpMo(CO)_3Cl]$ (**2**; 29.4 mg, 0.12 mmol) was added stepwise to a solution of TRIMEB (150 mg, 0.12 mmol) in dichloromethane (3 mL), allowing each fraction to dissolve before adding the next. The mixture was stirred for 2 h and then evaporated to dryness under reduced pressure to obtain a bright brick-red solid product. $(C_{63}H_{112}O_{35})\cdot(C_8H_5MoO_3Cl)\cdot 5H_2O$ (1800.1): calcd. C 47.37, H 7.11, Mo 5.33; found C 47.93, H 7.55, Mo 5.36. FTIR (KBr): $\tilde{\nu}$ = 3112 cm^{-1} m, 3101 m, 3094 m, 2979 vs, 2929 vs, 2831 s, 2050 vs, 1962 vs, 1941 vs, 1641 m, 1464 s, 1420 sh, 1404 m, 1368 m, 1322 m, 1303 m, 1258 sh, 1194 vs, 1161 vs, 1143 vs, 1109 vs, 1090 vs, 1073 vs, 1041 vs, 970 vs, 951 s, 910 m, 877 sh, 856 m, 838 w, 824 m, 785 w, 754 m, 736 m, 704 m, 658 w, 602 m, 564 s, 524 s, 470 m, 432 w, 419 sh, 407 m, 399 sh, 377 w, 357 w, 350 w. $^{13}C\{^1H\}$ CP/MAS NMR: δ = 99.8, 96.9, 92.8 (TRIMEB, C1), 85.5, 83.1, 82.3, 81.0, 78.6, 76.8 (TRIMEB, C2,3,4), 73.6, 72.6, 71.8, 70.6, 70.3, 69.8 (TRIMEB, C5,6), 63.2, 61.6, 60.9, 60.1, 59.3, 57.8, 56.7, 54.1 ppm (TRIMEB, O-CH_3).

Acknowledgments

This work was partly funded by the FCT, POCTI, and FEDER (project POCTI/CTM/46780/2002). We wish to thank Prof. João Rocha for access to research facilities and Paula Esculcas for assistance with the solid-state NMR experiments. We are also grateful to Celeste Azevedo for carrying out the TGA experiments and to Rosário Soares for collection of the powder diffraction data.

[1] a) J. Szejtli, *Chem. Rev.* **1998**, *98*, 1743–1754; b) W. Saenger, *Angew. Chem. Int. Ed. Engl.* **1980**, *19*, 344–362.

[2] a) W. Sliwa, T. Girek, *Heterocycles* **2003**, *60*, 2147–2183; b) E. Fenyvesi, L. Szente, N. R. Russel, M. McNamara, in *Comprehensive Supramolecular Chemistry* (Eds.: J. Szejtli, T. Osa), Pergamon, Oxford, **1996**, vol. 3, pp. 305–366; c) H. M. Colquhoun, J. F. Stoddart, D. J. Williams, *Angew. Chem. Int. Ed. Engl.* **1986**, *25*, 487–507.

[3] a) R. Breslow, G. Trainor, A. Ueno, *J. Am. Chem. Soc.* **1983**, *105*, 2739–2744; b) T. Matsue, D. H. Evans, T. Osa, N. Kobayashi, *J. Am. Chem. Soc.* **1985**, *107*, 3411–3417; c) A. Harada, S. Takahashi, *J. Chem. Soc., Chem. Commun.* **1984**, 645–648; d) A. Harada, Y. Hu, S. Yamamoto, S. Takahashi, *J. Chem. Soc., Dalton Trans.* **1988**, 729–732; e) Y. Odagaki, K. Hirotsu, T. Higuchi, A. Harada, S. Takahashi, *J. Chem. Soc., Perkin Trans. 1* **1990**, 1230–1231; f) Y. Liu, R.-Q. Zhong, H.-Y. Zhang, H.-B. Song, *Chem. Commun.* **2005**, 2211–2213; g) H. Ju, D. Leech, *Langmuir* **1998**, *14*, 300–306; h) A. E. Kaifer, *Acc. Chem. Res.* **1999**, *32*, 62–71; i) E. Coutouli-Argyropoulou, A. Kelaidopoulou, C. Sideris, G. Kokkinidis, *J. Electroanal. Chem.* **1999**, *477*, 130–139; j) D. Osella, A. Carretta, C. Nervi, M. Ravera, R. Gobetto, *Organometallics* **2000**, *19*, 2791–2797; k) J. A. Fernandes, S. Lima, S. S. Braga, P. Ribeiro-Claro, J. E. Rodriguez-

Borges, C. Teixeira, M. Pillinger, J. J. C. Teixeira-Dias, I. S. Gonçalves, *J. Organomet. Chem.* **2005**, *690*, 4801–4808; l) J. A. Fernandes, S. Lima, S. S. Braga, M. Pillinger, J. E. Rodríguez-Borges, P. Ribeiro-Claro, J. J. C. Teixeira-Dias, I. S. Gonçalves, *Eur. J. Inorg. Chem.* **2005**, 4729–4734; m) J. A. Fernandes, S. Lima, S. S. Braga, M. Pillinger, P. Ribeiro-Claro, J. E. Rodriguez-Borges, A. D. Lopes, J. J. C. Teixeira-Dias, I. S. Gonçalves, *Organometallics* **2005**, *24*, 5673–5677.

[4] a) I. Turel, A. Demšar, J. Košmrlj, *J. Inclusion Phenom.* **1999**, *35*, 595–604; b) S. S. Braga, I. S. Gonçalves, M. Pillinger, P. Ribeiro-Claro, J. J. C. Teixeira-Dias, *J. Organomet. Chem.* **2001**, *632*, 11–16; c) S. S. Braga, M. P. M. Marques, J. B. Sousa, M. Pillinger, J. J. C. Teixeira-Dias, I. S. Gonçalves, *J. Organomet. Chem.* **2005**, *690*, 2905–2912; d) J. Vinklárek, J. Honzícek, J. Holubová, *Central Eur. J. Chem.* **2005**, *3*, 72–81.

[5] G. Meister, H. Stoeckli-Evans, G. Süss-Fink, *J. Organomet. Chem.* **1993**, *453*, 249–253.

[6] B. Klingert, G. Rihs, *J. Chem. Soc., Dalton Trans.* **1991**, 2749–2760.

[7] a) M. Shimada, A. Harada, S. Takahashi, *J. Chem. Soc., Chem. Commun.* **1991**, 263–264; b) P. P. Patel, M. E. Welker, *J. Organomet. Chem.* **1997**, *547*, 103–112; c) C. Díaz, A. Arancibia, *J. Inclusion Phenom.* **1998**, *30*, 127–141; d) S. S. Braga, I. S. Gonçalves, P. Ribeiro-Claro, A. D. Lopes, M. Pillinger, J. J. C. Teixeira-Dias, J. Rocha, C. C. Romão, *Supramol. Chem.* **2002**, *14*, 359–366.

[8] D. R. Alston, A. M. Z. Slawin, J. F. Stoddart, D. J. Williams, *Angew. Chem. Int. Ed. Engl.* **1985**, *24*, 786–787.

[9] L. Song, Q. Meng, X. You, *J. Organomet. Chem.* **1995**, *498*, C1–C5.

[10] A. Harada, K. Saeki, S. Takahashi, *Organometallics* **1989**, *8*, 730–733.

[11] S. S. Braga, I. S. Gonçalves, A. D. Lopes, M. Pillinger, J. Rocha, C. C. Romão, J. J. C. Teixeira-Dias, *J. Chem. Soc., Dalton Trans.* **2000**, 2964–2968.

[12] S. Lima, I. S. Gonçalves, P. Ribeiro-Claro, M. Pillinger, A. D. Lopes, P. Ferreira, J. J. C. Teixeira-Dias, J. Rocha, C. C. Romão, *Organometallics* **2001**, *20*, 2191–2197.

[13] a) D. F. Eaton, A. G. Anderson, W. Tam, Y. Wang, *J. Am. Chem. Soc.* **1987**, *109*, 1886–1888; b) A. R. Dias, M. H. Garcia, M. P. Robalo, A. P. S. Tekheira, L. A. Bulygina, V. I. Sokolov, *Russ. J. Org. Chem.* **2001**, *37*, 620–623.

[14] P. M. Bersier, J. Bersier, B. Klingert, *Electroanalysis* **1991**, *3*, 443–455.

[15] L. Caron, H. Bricout, S. Tilloy, A. Ponchel, D. Landy, S. Fourmentin, E. Monflier, *Adv. Synth. Catal.* **2004**, *346*, 1449–1456.

[16] a) M. Abrantes, A. M. Santos, J. Mink, F. E. Kühn, C. C. Romão, *Organometallics* **2003**, *22*, 2112–2118; b) A. A. Valente, J. D. Seixas, I. S. Gonçalves, M. Abrantes, M. Pillinger, C. C. Romão, *Catal. Lett.* **2005**, *101*, 127–130.

[17] M. R. Caira, *Rev. Roumaine Chim.* **2001**, *46*, 371–386.

[18] H.-J. Schneider, F. Hacket, V. Rüdiger, H. Ikeda, *Chem. Rev.* **1998**, *98*, 1755–1785.

[19] a) L. Caron, C. Christine, S. Tilloy, E. Monflier, D. Landy, S. Fourmentin, G. Surpateanu, *Supramol. Chem.* **2002**, *14*, 11–20; b) L. Caron, S. Tilloy, E. Monflier, J. M. Wieruszeski, G. Lippens, D. Landy, S. Fourmentin, G. Surpateanu, *J. Inclusion Phenom.* **2000**, *38*, 361–379.

[20] V. Favre-Nicolin, R. Cerný, *J. Appl. Crystallogr.* **2002**, *35*, 734–743.

[21] V. Favre-Nicolin, R. Cerný, *FOX* – A Program for ab initio Structure Solution from Powder Diffraction Data, Program Developed for the Swiss National Science Foundation, University of Geneva, Switzerland, **2000**.

[22] M. Baranska, W. Łasocha, H. Kozłowski, L. M. Proniewicz, *J. Inorg. Biochem.* **2004**, *98*, 995–1001.

[23] R. Cerný, G. Renaudin, V. Favre-Nicolin, V. Hlukhyy, R. Pöttgen, *Acta Crystallogr., Sect. B* **2004**, *60*, 272–281.

[24] L. M. González-Méndez, F. L. Cumbrera, M. C. García-Cuesta, F. Sánchez-Bajo, A. L. Ortiz, F. J. Higes-Rolando, F. Luna-Giles, *Mater. Lett.* **2004**, *58*, 672–678.

[25] A. Grzechnik, V. Dmitriev, H.-P. Weber, J.-Y. Gesland, S. van Smaalen, *J. Phys.: Condens. Matter* **2004**, *16*, 1033–1043.

[26] E. M. Opozda, W. Łasocha, B. Włodarczyk-Gajda, *Z. Anorg. Allg. Chem.* **2004**, *630*, 597–603.

[27] a) Ž. Petrovski, S. S. Braga, S. S. Rodrigues, C. C. L. Pereira, I. S. Gonçalves, M. Pillinger, C. Freire, C. C. Romão, *New J. Chem.* **2005**, *29*, 347–354; b) Ž. Petrovski, S. S. Braga, A. M. Santos, S. S. Rodrigues, I. S. Gonçalves, M. Pillinger, F. E. Kühn, C. C. Romão, *Inorg. Chim. Acta* **2005**, *358*, 981–988.

[28] D. Mentzafos, I. M. Mavridis, H. Schenk, *Carbohydr. Res.* **1994**, *253*, 39–50.

[29] F. H. Allen, *Acta Crystallogr., Sect. B* **2002**, *58*, 380–388.

[30] F. H. Allen, W. D. S. Motherwell, *Acta Crystallogr., Sect. B* **2002**, *58*, 407–422.

[31] J. Laugier, B. Bochu, *CHECKCELL* – A Software Performing Automatic Cell/Space Group Determination, Collaborative Computational Project Number 14 (CCP14), Laboratoire des Matériaux et du Génie Physique de l'Ecole Supérieure de Physique de Grenoble (INPG), France, **2000**.

[32] J. Laugier, B. Bochu, *CELREF Version 3* – Cell Parameters Refinement Program from Powder Diffraction Diagram, Collaborative Computational Project Number 14 (CCP14), Laboratoire des Matériaux et du Génie Physique de l'Ecole Supérieure de Physique de Grenoble (INPG), France, **2000**.

[33] C. Bueno, M. R. Churchill, *Inorg. Chem.* **1981**, *20*, 2197–2202.

[34] P. Walters, M. Stahl, *BABEL Version 1.3* – A Program for the Interconversion of File Formats Used in Molecular Modelling, Department of Chemistry, University of Arizona, Tucson, AZ 85721, US, **1996**.

[35] A. March, *Z. Kristallogr.* **1932**, *81*, 285.

[36] W. A. Dollase, *J. Appl. Crystallogr.* **1986**, *19*, 267–272.

[37] J. Rodriguez-Carvajal, *FULLPROF* – A Program for Rietveld Refinement and Pattern Matching Analysis, Abstract of the Satellite Meeting on Powder Diffraction of the XV Congress of the IUCR, Toulouse, France, **1990**, p. 127.

[38] a) M. J. Gidley, S. M. Bociek, *J. Am. Chem. Soc.* **1988**, *110*, 3820–3829; b) S. J. Heyes, N. J. Clayden, C. M. Dobson, *Carbohydr. Res.* **1992**, *233*, 1–14.

[39] R. P. Veregin, C. A. Fyfe, R. H. Marchessault, M. G. Tayler, *Carbohydr. Res.* **1987**, *160*, 41–56.

[40] L. Cunha-Silva, J. J. C. Teixeira-Dias, *New J. Chem.* **2005**, *29*, 1335–1341.

[41] G. R. Brown, M. R. Caira, L. R. Nassimbeni, B. van Oudtshoorn, *J. Inclusion Phenom.* **1996**, *26*, 281–294.

[42] J. K. P. Ariyaratne, A. M. Bierrum, M. L. H. Green, M. Ishaq, C. K. Prout, M. G. Swanwick, *J. Chem. Soc. A* **1969**, 1309.

Received: November 11, 2005
Published Online: February 28, 2006

